THE JOURNAL OF PHYSICAL CHEMISTRY B LETTERS

2008, *112,* 12571–12574
Published on Web 10/01/2008

Solvent Effect of Alcohols at the L-Edge of Iron in Solution: X-ray Absorption and Multiplet Calculations

Sébastien Bonhommeau,[†] Niklas Ottosson,[†,‡] Wandared Pokapanich,[‡] Svante Svensson,[‡] Wolfgang Eberhardt,[†] Olle Björneholm,[‡] and Emad F. Aziz*[,†]

BESSY GmbH., Albert-Einstein-Strasse 15, 12489 Berlin, Germany, and Department of Physics and Materials Science, Uppsala University, Box 530, SE-751 21 Uppsala, Sweden

Received: August 9, 2008; Revised Manuscript Received: September 16, 2008

The local electronic structure of Fe(III) and Fe(II) ions in different alcohol solutions (methanol, ethanol, propan-1-ol) is investigated by means of soft X-ray absorption spectroscopy at the iron $L_{2,3}$-edge. The experimental spectra are compared with ligand field multiplet simulations. The solvated Fe(III) complex is found to exhibit octahedral symmetry, while a tetragonal symmetry is observed for Fe(II). A decrease in the solvent polarity increases the charge transfer from the oxygen of the alcohol to the iron ions. This conclusion is supported by Hartree−Fock calculations of the Mulliken charge distribution on the alcohols. A larger charge transfer is further observed from the solvent to Fe(III) compared to Fe(II), which is connected to the higher positive charge state of the former. Finally, iron ions in solution are found to prefer the high-spin configuration irrespective of their oxidation state.

1. Introduction

The solvated structure of ions plays a key role for their reactivity.[1,2] Spectroscopic techniques have shed light on the intricate nature of ion solvation and quantified the ion−solvent bond length and coordination number. Among them, Raman spectroscopy provides detailed information on the symmetry of metal−oxygen stretching frequencies in solution. However, the sample should be highly concentrated in order to obtain a reasonable signal-to-noise ratio.[3] Another highly useful technique is extended X-ray absorption fine structure (EXAFS), which has become one of the most powerful tools to determine structural features of ions in solution.[4] Combined with molecular dynamics simulations, EXAFS measurements have provided a detailed picture of the solvated structure of many transition metal ions.[5] In most cases, EXAFS is performed on a hard X-ray K-level, with typical linewidths belonging to the 1−2 eV range.[6] $L_{2,3}$-edge X-ray absorption spectroscopy (XAS) has also attracted a lot of interest as a tool to study transition metals. $L_{2,3}$-edge spectra correspond to dipole-allowed $2p \rightarrow 3d$ transitions (with intrinsic linewidths in the 300−700 meV energy range) which results in stronger and more structured absorption features than at the K-edge. Furthermore, 2p−3d Coulomb and exchange interactions cause $L_{2,3}$-edges to show a multiplet structure which is very sensitive to the metal nature and coordination. Cramer et al. have performed L-edge XAS on biorelevant systems such as proteins where transition metals occupy the active center.[7,8] Nonetheless, as measurements below 1 keV require ultrahigh vacuum (UHV), the hydrated samples had to be frozen in these studies.

Recent developments at soft X-ray facilities have made it possible to investigate high-pressure samples (e.g., volatile solution) in new ways.[9−12] This has allowed us to record $L_{2,3}$-edge XA spectra of transition metals in aqueous solution and study systems in low concentration (below 100 mM).[13] In this Letter, we investigate the $L_{2,3}$-edge of Fe(II) and Fe(III) in different alcohol solutions by XAS. The experimental results are compared with multiplet simulations, providing a detailed picture of the solvated structure of Fe(II) and Fe(III) as well as the solvent-to-metal charge transfer efficiency in the different solutions.

2. Methods

2.a. Experimental Details. The iron $L_{2,3}$-edge XAS measurements were conducted at the U41-PGM high-flux undulator beamline at BESSY, Berlin, Germany. The setup has previously been described.[13,14] Briefly, the solution circulates in an UHV chamber inside a stainless steel tubing at a speed of 1 L/min, constantly providing a renewed sample. The liquid sample is irradiated by the soft X-ray radiation behind a 150 nm thick Si_3N_4 membrane. Absorption is determined by measuring the total fluorescence yield (TFY) using a 5×5 mm^2 GaAsP photodiode, at an angle of 45° in the polarization plane. Due to the relatively long attenuation length of soft X-rays in condensed matter, being on the order of a micron, the detection method is primarily bulk sensitive. The resolution of the experiment was better than 200 meV at 700 eV photon energy.

The samples were prepared fresh before each experiment from highly purified, commercially available anhydrous $FeCl_2$ and $FeCl_3$ (>99.8%, Sigma-Aldrich). The salt concentrations were in all cases 500 mM, at which spectral saturation and ion pairing are weak.[13] $FeCl_3$ was solvated in three different solvents,

* To whom correspondence should be addressed. E-mail: Emad.Aziz@bessy.de.
[†] BESSY GmbH.
[‡] Uppsala University.

10.1021/jp8071266 CCC: $40.75

namely, methanol, ethanol, and propan-1-ol. $FeCl_2$ was only prepared in methanol and ethanol, due to its low solubility in propan-1-ol.

2.b. Theoretical Details. $L_{2,3}$-edge absorption spectra were modeled using ligand field multiplet (LFM) theory.[15−17] The effects of σ- and π-donation from the alcohol solvents were accounted for by including ligand-to-metal charge transfer (LMCT) in the simulations. The ground state of a $3d^n$ ion was accordingly taken to be a linear combination of two appropriate configurations, $3d^n$ and $3d^{n+1}\underline{L}$, where $3d^{n+1}\underline{L}$ denotes the configuration with an extra 3d electron coming from the solvent ligand and with a corresponding hole on a ligand orbital. Since the ion pair formation of iron with chloride is weak at the concentration studied here, the configurations where a counterion acts as a ligand were not considered in the simulations. Octahedral surroundings of the metal ions were represented by octahedral (O_h) crystal field potentials, whose strength was parametrized by 10Dq. For a tetragonal (D_{4h}) crystal field, two additional parameters, Ds and Dt, must be included to account for the distortion of the coordination sphere. In order to compare the theoretically obtained discrete transition probabilities with the experimental $L_{2,3}$-edge XA spectra, they must be broadened. A Lorentzian broadening function was therefore applied to the simulated spectra which accounts for the intrinsic lifetime of the core hole, while a Gaussian broadening function describes the finite instrumental resolution (details for the theoretical parameters are presented in Supporting Information Table S1).

In order to calculate the electron density at the oxygen site of the alcohol solvents, Hartree−Fock (HF) calculations have been performed for each molecule, using the 6-311G** basis set and the Gaussian 03 program package.[18] The solvent was modeled as a polarizable continuum (called the reaction field), described by a uniform dielectric constant, where the solute is embedded into a cavity within the solvent. We have used Tomasi's polarized continuum model (PCM), where the cavity is constructed from a series of interlocking atomic spheres.[19] From the optimized structures, the respective Mulliken charge distributions were obtained.

3. Results and Discussion

Figure 1a presents XA spectra of 500 mM $FeCl_3$ in various alcohols, namely, methanol (red full line), ethanol (green dashed line), and propan-1-ol (black dotted line). Upon increasing the alcohol chain length, the main peak of the L_3-edge at 710.1 eV (*A*, see Figure 1 inset) shifts progressively toward lower energies. For ethanol, it shifts by 200 meV and for propan-1-ol by 300 meV, relative to methanol. The prepeak of the L_3-edge appears at 709.0 eV, and increases slightly in intensity upon changing the solvent from methanol to ethanol, while a significant increase in intensity is observed for the propan-1-ol solution. Another peak appears on the high-energy side of the L_3-edge, at 715.4 eV, which shows a systematic decrease in intensity upon changing the solvent from methanol to propan-1-ol.

At the Fe(III) L_2-edge, a prepeak appears at approximately 720.7 eV and progressively increases in intensity with increasing alcohol chain length, similar to what is observed at the L_3-edge. On the other hand, the magnitude of the intensity change at the prepeak of the L_2-edge is quite different from that at the L_3-edge. The L_2-edge of the methanol solution is composed of two main peaks at 722.3 eV (*B*, see Figure 1 inset) and 723.7 eV. Similar to the *A*-peak at the L_3-edge, a systematic shift and intensity variation is observed at the *B*-peak as a function of the solvent. The edge shifts by 100 meV to lower energies upon changing the solvent from methanol to ethanol and by 300 meV when changing the solvent from methanol to propan-1-ol. This is accompanied by a decrease in intensity of the high-energy feature relative to the low-energy one, when going from methanol to propan-1-ol. From these observations, we can conclude that lengthening the alkyl chains of the alcohol solvents does not linearly affect the local electronic structure of the solvated Fe(III) ions. While propan-1-ol induces a significant effect at the $L_{2,3}$-edge of Fe(III) compared to ethanol, the observed difference when going from methanol to ethanol is much less pronounced.

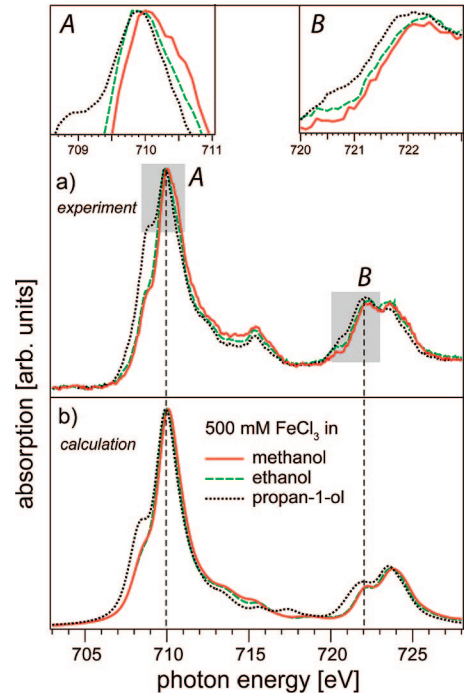

Figure 1. (a) Experimental XA spectra of $FeCl_3$ in methanol (red solid curve), ethanol (green dashed curve), and propan-1-ol (black dotted curve). (b) Corresponding LFM simulations in O_h symmetry with the same color code. The *A* and *B* insets are discussed in the text.

The experimentally observed changes in the Fe(III) XA spectra upon changing solvent are qualitatively reproduced in our ligand field multiplet simulations, presented in Figure 1b. The calculated spectra exhibit the observed experimental trends; i.e., they show a stronger effect at the L_3-edge than at the L_2-edge. The ground-state configurations found to be in best agreement with the experimental data are 75% d^5 + 25% $d^6\underline{L}$ for $FeCl_3$ in methanol, 71% d^5 + 29% $d^6\underline{L}$ for $FeCl_3$ in ethanol, and 60% d^5 + 40% $d^6\underline{L}$ in propan-1-ol, The contribution of the charge transfer configuration is consequently increasing upon raising the electron-donor strength of the solvent. Our HF calculations performed on methanol, ethanol, and propan-1-ol, as shown in Figure 2, suggest that the bigger the alcohol is, the larger the effective negative charge is at the oxygen site. Note, however, that these calculations only consider a single alcohol molecule in a polarizable continuum, whereas iron ions in solution are on average surrounded by six alcohol molecules in the first hydration shell, constituting an O_h field. Altogether, this suggests a stronger reactivity of the oxygen in propan-1-ol compared to ethanol and in ethanol relative to methanol and explains the increase in LMCT on going from methanol to propan-1-ol solvation. This is also in accord with the well-known decrease in dielectric constant when lengthening the alkyl chain of alcohols ($\varepsilon_{methanol} = 33$, $\varepsilon_{ethanol} = 24.3$, and $\varepsilon_{propan\text{-}1\text{-}ol} = 20.1$). Because of dielectric shielding, the attractive force between

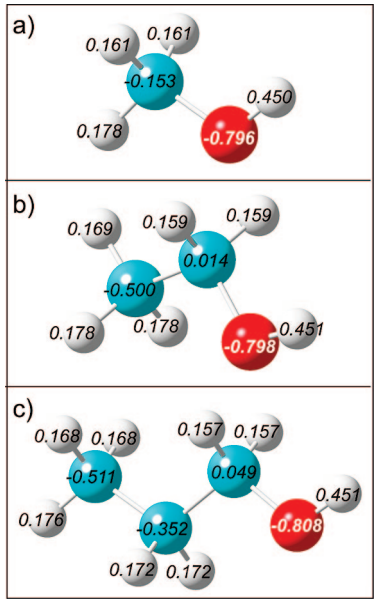

Figure 2. Mulliken charge distributions on pure alcohol solvents, namely, (a) methanol, (b) ethanol, and (c) propan-1-ol, as obtained from HF calculations employing a PCM field. As discussed in the text, this quantity correlates to the solvent-to-ion charge transfer efficiency.

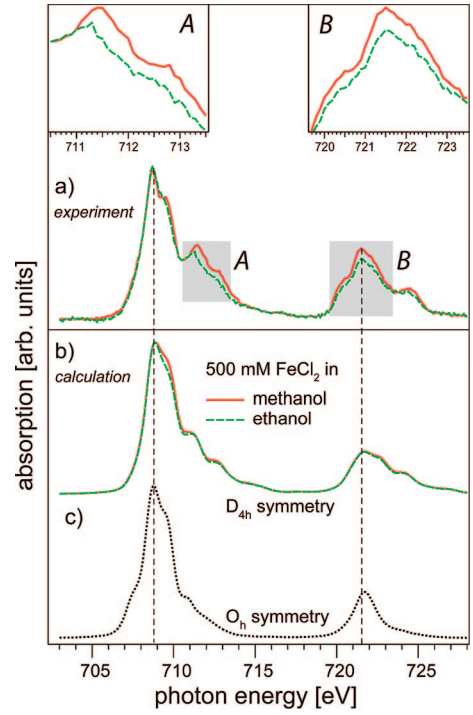

Figure 3. (a) Experimental XA spectra of $FeCl_2$ in two solvents, namely, methanol (red solid curve) and ethanol (green dashed curve). (b) Corresponding LFM simulations in D_{4h} symmetry with the same color code. (c) Best agreement between LFM simulation and experiment in O_h symmetry. The *A* and *B* insets are discussed in the text.

opposite charges is inversely proportional to the dielectric constant.[20] As a consequence, the strongest LMCT to the Fe(III) ions is expected for solvents with the lowest dielectric constants, i.e., for the least polar alcohol molecules. At this point, it is worth mentioning that, even if the iron molecular orbitals are affected by the solvent, no change in 2p spin−orbit splitting has been observed upon changing alcohol solvent. In addition, the best agreement between experimental data and simulations is always obtained in O_h symmetry for solvated Fe(III) ions. A tetragonal symmetry was also tested, to account for some distortion of the O_h coordination sphere, but did not improve the accordance between theory and experiment.

The experimental L-edge XA spectra of 500 mM $FeCl_2$ in different alcohol solvents are presented in Figure 3a. The L_3-edge of the methanol solution is characterized by two main peaks at 708.7 and 709.3 eV, followed by two multiplet peaks at 711.5 and 712.8 eV (*A*, see Figure 3 inset). Upon replacing methanol by ethanol, the latter two are both shifted by approximetaly 200 meV to lower energy. The L_2-edge consists of three main peaks, at approximately 720.4, 721.5 (*B*, see Figure 3 inset), and 724.3 eV. For the ethanol solution, the intensity of the L_2-edge decreases significantly relative to the L_3-edge, compared to the methanol solution. To explain the origin of these experimental observations, LFM simulations have been carried out for Fe(II) ions in the two alcohol solvents, as shown in Figure 3b. The spectral features are quite well reproduced. However, even though the change observed experimentally upon substituting the solvent nicely matches the calculation at the L_3-edge, the agreement at the L_2-edge is poorer. The LFM calculations again show an increase in LMCT for ethanol compared to methanol as for the Fe(III) case. The ground-state configurations for these systems are 84% d^6 + 16% $d^7\underline{L}$ for $FeCl_2$ in methanol and 82% d^6 + 18% $d^7\underline{L}$ for $FeCl_2$ in ethanol The charge transfer contribution appears to be weaker than for $FeCl_3$ (25% $d^6\underline{L}$ for $FeCl_3$ but only 16% $d^7\underline{L}$ for $FeCl_2$ in methanol and 29% $d^6\underline{L}$ for $FeCl_3$ but only 18% $d^7\underline{L}$ for $FeCl_2$ in ethanol) which is expected due to the lower positive charge state of Fe(II) compared to Fe(III). Interestingly, the best agreement with experimental data is obtained in D_{4h} symmetry. In O_h symmetry, the calculated spectrum is definitely not in agreement with the experimental one (see Figure 3c). In addition, we note that the distortion is a bit weaker in the methanol solution (10Dq = 0.4 eV, Dt = 0.11 eV, Ds = 0) than in ethanol (10Dq = 0.4 eV, Dt = 0.13 eV, Ds = 0), most likely due to the smaller size of methanol molecules.

In all solutions studied here, Fe(II) and Fe(III) are found to remain in their respective high-spin state. This can be inferred from the low crystal fields, 10Dq ≤ 1.0 eV, giving the best agreement between theory and experiments (see Supporting Information Table S1). A low-spin Fe(III) ion would present a distinct peak on the low-energy side of the L_3-edge corresponding to the transition $2p^6t_{2g}^5e_g^0 \rightarrow 2p^5t_{2g}^6e_g^0$. This is clearly not observed experimentally, and thus strongly suggests that the system is in a high-spin configuration.[21] Regarding Fe(II) ions, our XA spectra resemble those of high-spin ferrous materials reported earlier in the solid state.[22] In particular, the L_2-edge of the spectra reported in ref 22 is almost identical to what has been observed in this study but very different from what is expected in the low-spin state.[22] The high-spin state of iron ions in solution are stabilized by the weak chemical pressure of the alcohol molecules. The induced weak ligand field leads to the population of the Fe antibonding e_g orbitals (in O_h symmetry), and the Fe−solvent bonds are consequently longer than those in the low-spin state (requiring a stronger chemical pressure to be stabilized). In the solid state, iron chloride ions such as $[FeCl_6]^{3-}$ and $[FeCl_6]^{4-}$ are still in the high-spin state but their cubic crystal field is somewhat higher than what is observed for Fe(II) and Fe(III) in solution (10Dq = 1.2 eV for $[FeCl_6]^{3-}$ and 10Dq = 0.6 eV for $[FeCl_6]^{4-}$).[22] It is however difficult to accurately compare the iron ions in solution with those in the solid state due to the weak ion pairing with the chloride anions in the former. More quantitative data can potentially be obtained

by comparing Fe complexes whose ligands remain coordinated to the iron center in solution.

4. Conclusion

The $L_{2,3}$-edge of iron ions in different alcohol solutions has been investigated by X-ray absorption spectroscopy for the first time. Due to the high sensitivity of the L-edge to the nature and symmetry of the surrounding ligands, effects of varying the alcohol solvent are clearly reflected in the spectra. The solvated Fe(III) ions have been found to exhibit an O_h symmetry, while the Fe(II) ligand field seems to be more distorted. In the case of solvated Fe(II) ions, a D_{4h} symmetry has been evidenced. By comparing the experimental spectra of Fe(III) and Fe(II) ions in solution with LFM theory calculations, we have further quantified the charge transfer efficiency in the different solvents. Finally, we have shown that iron ions in alcohol solution prefer the high-spin state, independent of their oxidation state. The present study motivates future work on aqueous and physiological solutions of biologically relevant materials, where the transition metal occupies the active center.

Supporting Information Available: Table showing the ground-state configurations and ligand field multiplet parameters used to simulate experimental XA spectra of $FeCl_3$ and $FeCl_2$. This material is available free of charge via the Internet at http://pubs.acs.org.

References and Notes

(1) Richens, D. T. *The Chemistry of Aqua Ions: Synthesis, Structure and Reactivity: A Tour Through the Periodic Table of the Elements*, 1st ed.; Wiley: New York, 1997.

(2) Chazin, W. J. *Nat. Struct. Biol.* **1995**, *2*, 707.

(3) Kanno, H. *J. Phys. Chem.* **1988**, *92*, 4232.

(4) Sham, T. K.; Hastings, J. B.; Perlman, M. L. *J. Am. Chem. Soc.* **1980**, *102*, 5904.

(5) D'Angelo, P.; Barone, V.; Chillemi, G.; Sanna, N.; Meyer-Klaucke, W.; Pavel, N. V. *J. Am. Chem. Soc.* **2002**, *124*, 1958.

(6) Stöhr, J. *NEXAFS spectroscopy*; Springer-Verlag: Berlin, New York, 1992.

(7) Cramer, S. P.; Peng, G.; Christiansen, J.; Chen, J.; vanElp, J.; George, S. J.; Young, A. T. *J. Electron Spectrosc. Relat. Phenom.* **1996**, *78*, 225.

(8) Cramer, S. P.; Ralston, C. Y.; Wang, H. X.; Bryant, C. *J. Electron Spectrosc. Relat. Phenom.* **1997**, *86*, 175.

(9) Smith, J. D.; Cappa, C. D.; Wilson, K. R.; Messer, B. M.; Cohen, R. C.; Saykally, R. J. *Science* **2004**, *306*, 851.

(10) Wernet, P.; Nordlund, D.; Bergmann, U.; Cavalleri, M.; Odelius, M.; Ogasawara, H.; Näslund, L. A.; Hirsch, T. K.; Ojämae, L.; Glatzel, P.; Pettersson, L. G. M.; Nilsson, A. *Science* **2004**, *304*, 995.

(11) Guo, J. H.; Luo, Y.; Augustsson, A.; Kashtanov, S.; Rubensson, J. E.; Shuh, D. K.; Agren, H.; Nordgren, J. *Phys. Rev. Lett.* **2003**, *91*, 157401.

(12) Aziz, E. F.; Ottosson, N.; Faubel, M.; Hertel, I. V.; Winter, B. *Nature* **2008**, *455*, 89.

(13) Aziz, E. F.; Eisebitt, S.; de Groot, F.; Chiou, J.; Dong, C.; Guo, J.; Eberhardt, W. *J. Phys. Chem. B* **2007**, *111*, 4440.

(14) Aziz, E. F.; Freiwald, M.; Eisebitt, S.; Eberhardt, W. *Phys. Rev. B* **2006**, *73*, 75120.

(15) Cowan, R. D. *J. Opt. Soc. Am.* **1968**, *58*, 808.

(16) Butler, P. H. *Point Group Symmetry, Applications, Methods and Tables*; Plenum: New York, 1991.

(17) de Groot, F. M. F. *Coord. Chem. Rev.* **2005**, *249*, 31.

(18) Frisch, M. J.; Trucks, G. W.; Schlegel, H. B.; Scuseria, G. E.; Robb, M. A.; Cheeseman, J. R.; Zakrzewski, V. G.; Montgomery, J. A.; Stratmann, R. E.; Burant, J. C.; Dapprich, S.; Millam, J. M.; Daniels, A. D.; Kudin, K. N.; Strain, M. C.; Farkas, O.; Tomasi, J.; Barone, V.; Cossi, M.; Cammi, R.; Mennucci, B.; Pomelli, C.; Adamo, C.; Clifford, S.; Ochterski, J.; Petersson, G. A.; Ayala, P. Y.; Cui, Q.; Morokuma, K.; Salvador, P.; Dannenberg, J. J.; Malick, D. K.; Rabuck, A. D.; Raghavachari, K.; Foresman, J. B.; Cioslowski, J.; Ortiz, J. V.; Baboul, A. G.; Stefanov, B. B.; Liu, G.; Liashenko, A.; Piskorz, P.; Komaromi, I.; Gomperts, R.; Martin, R. L.; Fox, D. J. Keith, T.; Al-Laham, M. A.; Peng, C. Y.; Nanayakkara, A.; Challacombe, M.; Gill, P. M. W.; Johnson, B.; Chen, W.; Wong, M. W.; Andres, J. L.; Gonzalez, C.; Head-Gordon, M.; Replogle, E. S.; Pople, J. A. Gaussian 03, Windows 03 ed.; Gaussian, Inc. Pittsburgh, PA, 2003.

(19) Cossi, M.; Barone, V.; Cammi, R.; Tomasi, J. *Chem. Phys. Lett.* **1996**, *255*, 327.

(20) Wang, Z.; Friedrich, D. M.; Ainsworth, C. C.; Hemmer, S. L.; Joly, A. G.; Beversluis, M. R. *J. Phys. Chem. A* **2001**, *105*, 942.

(21) Hocking, R. K.; Wasinger, E. C.; de Groot, F. M. F.; Hodgson, K. O.; Hedman, B.; Solomon, E. I. *J. Am. Chem. Soc.* **2006**, *128* 10442.

(22) Wasinger, E. C.; de Groot, F. M. F.; Hedman, B.; Hodgson, K. O.; Solomon, E. I. *J. Am. Chem. Soc.* **2003**, *125*, 12894.

JP8071266